

## **Industrial wastewater volume reduction through osmotic concentration: Membrane module selection and process modeling**

Joel Minier-Matar, Mashael Al-Maas, Dareen Dardor, Arnold Janson, Mustafa S. Nasser, Samer Adham

### **Item type**

Journal Contribution

### **Terms of use**

This work is licensed under a [CC BY 4.0](https://creativecommons.org/licenses/by/4.0/) license

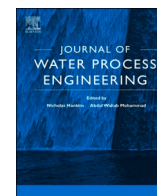
### **This version is available at**

[https://manara.qnl.qa/articles/journal\\_contribution/Industrial\\_wastewater\\_volume\\_reduction\\_through\\_osmotic\\_concentration\\_Men](https://manara.qnl.qa/articles/journal_contribution/Industrial_wastewater_volume_reduction_through_osmotic_concentration_Men)

Access the item on Manara for more information about usage details and recommended citation.

**Posted on Manara – Qatar Research Repository on**

2021-04-01



# Industrial wastewater volume reduction through osmotic concentration: Membrane module selection and process modeling

Joel Minier-Matar<sup>a,\*</sup>, Mashaël Al-Maas<sup>a</sup>, Dareen Dardor<sup>a</sup>, Arnold Janson<sup>a</sup>, Mustafa S. Nasser<sup>b</sup>, Samer Adham<sup>a,c,\*</sup>

<sup>a</sup> ConocoPhillips Global Water Sustainability Centre, Qatar Science & Technology Park, Doha, Qatar

<sup>b</sup> Gas Processing Centre, College of Engineering, Qatar University, Doha, Qatar

<sup>c</sup> Center of Advanced Materials, Qatar University, Doha, Qatar

## ARTICLE INFO

### Keywords:

Osmotic concentration  
Forward osmosis  
Wastewater treatment  
Oil and gas  
Seawater  
Bench scale  
Pilot plant

## ABSTRACT

Osmotic concentration (OC), a form of forward osmosis (FO) but without draw solution recovery, can be applied for reducing wastewater disposal volumes in the oil & gas industry. Within this industry, wastewater is often disposed of by injection through disposal wells into deep underground reservoirs. By reducing wastewater disposal volumes, the sustainability of the disposal reservoir is improved. In this application of OC, seawater or brine from a desalination plant serves as the draw solution and the diluted seawater is discharged to the sea. This study compared 3 commercial hollow-fiber FO membranes (CTA, TFC, aquaporin proteins) for reducing the volume of low salinity wastewater generated during liquified natural gas (LNG) production. Additionally, a model was developed to predict the performance of commercial full-scale membranes by identifying optimum operating conditions, taking into consideration the trade-off between feed concentration factor and water flux. Bench-scale tests were conducted using synthetic and actual wastewater from an LNG facility to evaluate OC technology performance and validate model predictions.

Based on model results with a feed mimicking the salinity of actual wastewater, a 4x concentration factor produced a reasonable compromise between feed recovery and draw solution dilution and was considered the optimum for future tests. At higher concentration factors, the increased dilution of the draw solution negatively impacted flux. In bench tests with real wastewater, the TFC chemistry had a  $\approx 5x$  higher water flux (9.7 vs. 1.9 L/m<sup>2</sup>-h) and a  $\approx 3x$  lower specific reverse solute flux (192 vs. 551 mg/L) compared to the CTA chemistry. However, both membranes showed less than 5% fouling and a specific forward organic solute flux of less than 0.5 mg/L of total organic carbon (TOC). Pilot testing for >50 h showed stable performance, comparable to bench scale data and model predictions.

## 1. Introduction

Oil and gas (O&G) are considered to be integral energy sources for growing economies around the world [1–3]. Nevertheless, the production of O&G is associated with large volumes of water that must be managed appropriately. Water produced in O&G upstream operations is referred to as produced water (PW) and water generated as a byproduct from hydrocarbon refining is described as process water [4]. It has been estimated that, on average, about 3–4 barrels of PW are generated for every barrel of oil extracted from conventional operations [4]. This ratio depends on multiple factors including hydrocarbon reservoir type, geology, and age, and could reach up to 10 barrels of water for each barrel

of oil in older production wells [5]. With such large volumes of wastewater being handled by O&G companies daily, effective water management is vital concern for maintaining economically feasible development of O&G fields [6].

Although treatment for surface discharge or reuse can be applied, direct injection into disposal wells continues to be the primary approach for water management [2,7]. This practice faces several challenges since a disposal well has only limited capacity and the costs for well drilling and maintenance are significant [2,8]. By reducing the volume of wastewater sent to disposal, the service life of a well can be dramatically improved and deferring or eliminating the disposal well drilling costs can be an important factor in calculating life-cycle cost-effectiveness of

\* Corresponding authors.

E-mail addresses: [Joel.e.miniermatar@conocophillips.com](mailto:Joel.e.miniermatar@conocophillips.com) (J. Minier-Matar), [sadham@qu.edu.qa](mailto:sadham@qu.edu.qa) (S. Adham).

<https://doi.org/10.1016/j.jwpe.2020.101760>

Received 14 September 2020; Received in revised form 18 October 2020; Accepted 19 October 2020

Available online 4 November 2020

2214-7144/© 2021 The Authors. Published by Elsevier Ltd. This is an open access article under the CC BY license (<http://creativecommons.org/licenses/by/4.0/>).

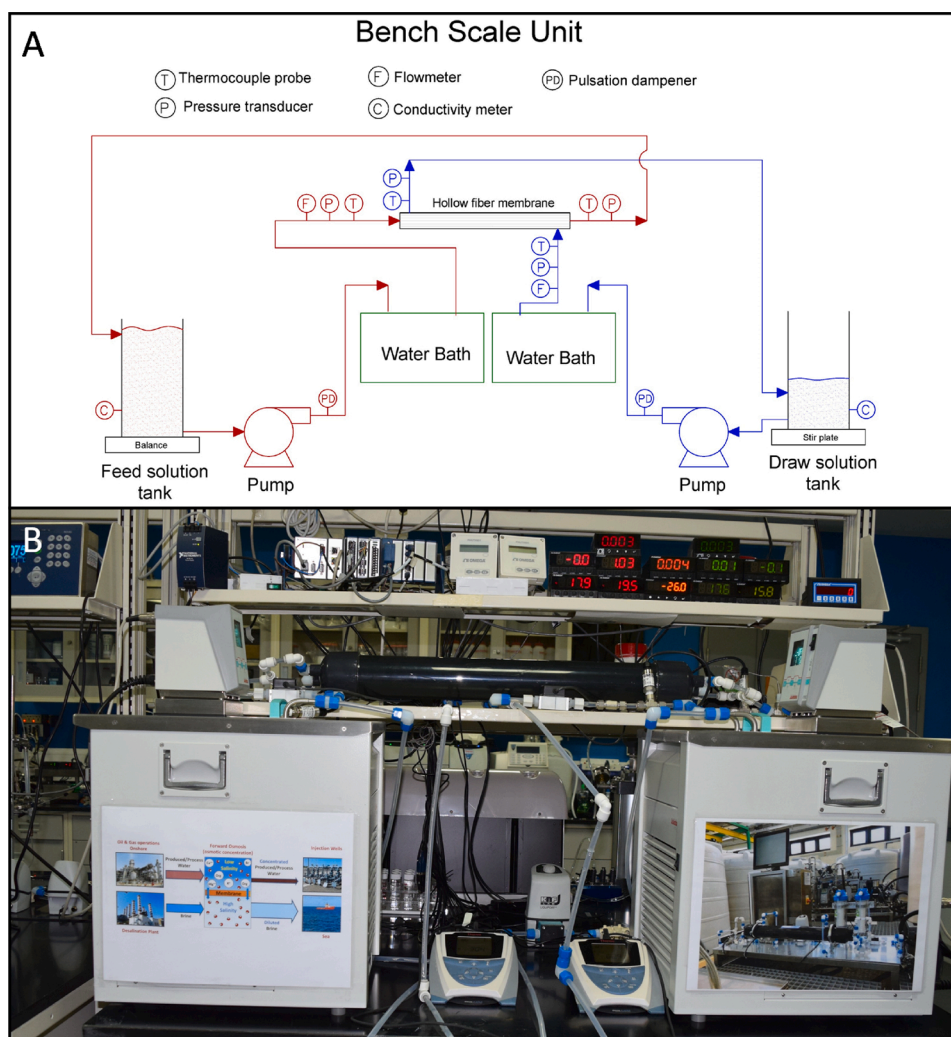


Fig. 1. Osmotic concentration bench-scale unit A) Schematic and B) Photo.

water treatment. In selecting a treatment technology, the water quality and need for water reuse has to be considered [9–14]. Gas field produced waters are typically characterized by their low salinity, typically <5000 mg/L [4,15], making them attractive for treatment for recycling opportunities and/or volume reduction prior to disposal. Examples of O&G installations adopting advanced technologies to treat wastewater streams include:

- In Qatar, membrane bioreactor (MBR) and reverse osmosis (RO) technologies were integral to reducing injection volumes and providing fresh water for LNG operations [15]
- In Australia, RO has been applied to treat coal seam gas wastewater for beneficial reuse, including agriculture [16].

When coupled with integrity monitoring techniques, osmotic concentration (OC) can be applied as a technology for produced and process water (PPW) volume reduction [17,18]. Like forward osmosis (FO), OC uses semi-permeable membranes and is considered an “osmotic process”. In both OC & FO, mass transfer is driven by an osmotic pressure differential between a low salinity feed solution (FS), e.g. wastewater, and a high salinity draw solution (DS), e.g. seawater [19–23]. The distinction is that in FO, the objective is typically to recover the water that passes through the membrane [24] while in OC, the objective is to concentrate the feed stream [2,25–27]. In contrast with reverse osmosis (RO) which operates at elevated pressures, OC & FO operate at ambient pressures and rely simply on diffusion for mass transfer [2]. Key

advantages of osmotic processes over RO include lower capital and operating expenses and lower fouling tendencies [28–33]. In recent years, these advantages, together with improvements in flat sheet and hollow fiber osmotic membranes, have increased the potential of FO & OC for wastewater treatment and seawater desalination [2,28,34–37]. In comparison with RO & FO, the disadvantage of OC is that there is no water production.

In previous studies, OC’s technical feasibility to reduce the volume of a gas field PPW by 50 % was validated in bench scale tests [25,26]. These studies showed stable flux and excellent rejection of the organics present in the process water. One key aspect to scale-up OC for field implementation is to identify suitable full-scale membrane modules capable of treating PPW with minimal fouling and stable long-term operation [38]. The hollow-fiber membrane configuration performance was proven in the bench scale study [26] and was selected for this investigation. Compared to spiral wound and flat sheet configurations, the key advantages of hollow fiber membranes include [39,40]:

- Higher packing density minimizes equipment footprint
- Better hydrodynamics produces high fluxes

Another important aspect for OC scale-up is the development of accurate models to forecast membrane performance [41]. Many models have been already developed for predicting performance of small membrane modules [19,42–49]. For larger modules, there are certain limitations since those models are not able to predict the expected feed

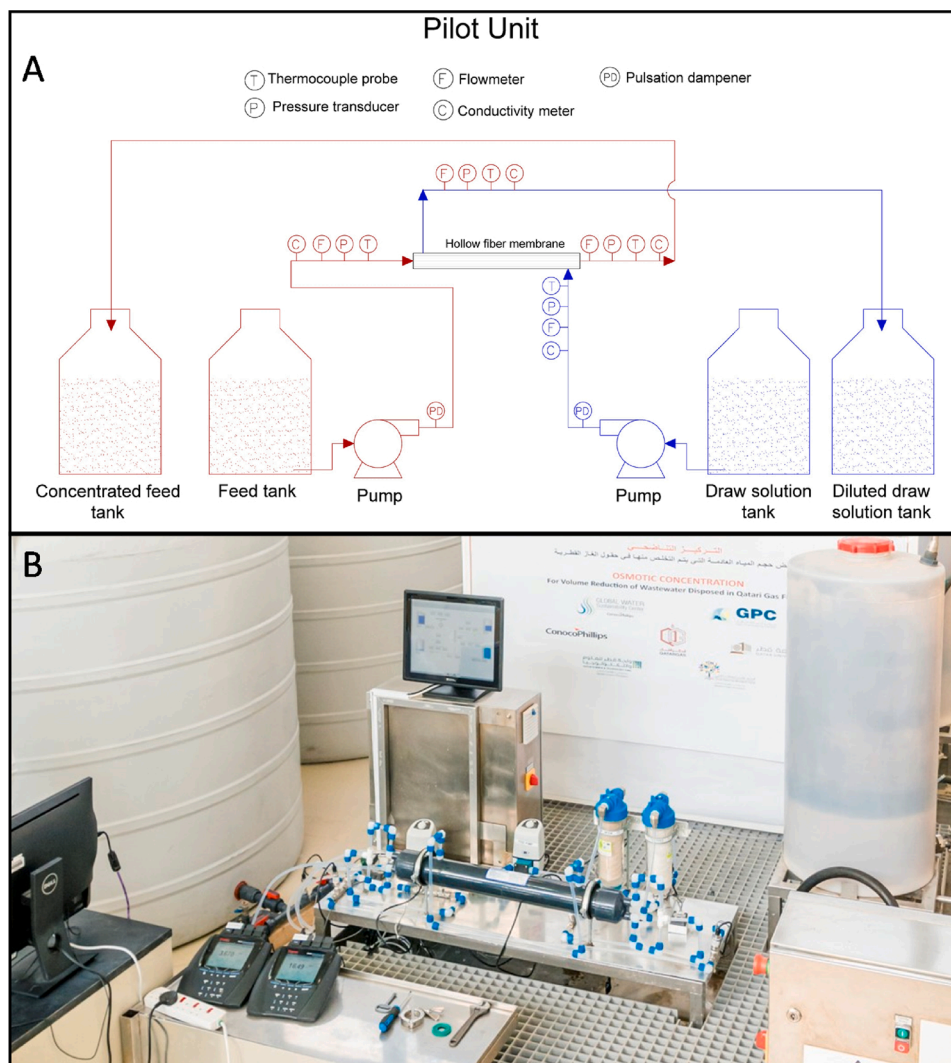


Fig. 2. Osmotic concentration pilot unit A) Schematic and B) Photo.

recovery or draw solution dilution needed. Also, those models do not account for the variations in the feed and draw concentrations as the solutions flow through a module. Other models target the design and optimization of FO systems, which include details about full-scale modules [50–52]. However, those models focused mainly on designs and not on individual commercial module performance and those models are not available for public use.

The primary aims of this paper are to:

- Screen and identify commercial hollow-fiber FO membranes suitable for the treatment of wastewater generated during natural gas processing
- Develop a comprehensive model capable of predicting the performance of commercial modules based on the operating conditions, feed recovery and draw solution dilution.
- Validate bench scale membrane performance data using pilot-scale system.

To the authors' knowledge, this is the first time that the performance of commercial hollow-fiber osmotic membranes has been compared for the reduction of process water disposal volumes within the oil and gas industry.

## 2. Materials and methods

### 2.1. FO testing systems

#### 2.1.1. Bench scale unit

The osmotic concentration unit (Fig. 1) used to evaluate commercial module performance consisted of two independent closed loops for the feed and draw solutions. The flow rates were controlled by two diaphragm positive displacement pumps (NF-1300, KNF, Switzerland) and kept constant using a PID controller embedded within the LabVIEW real-time control system (cRIO 9068, National Instruments, USA). The water flux across the membrane was measured using a digital balance to record the feed solution change in weight with time (Meter Toledo, USA). The temperature within the loop was maintained constant using a refrigerated/heating circulator (Julabo, Germany). The main process parameters of pressure, temperature, flow, and conductivity were monitored and recorded. To keep the draw solution constant during the bench scale test, the volume of the draw solution was at least 10 times larger than the volume permeating through the membrane to limit the draw solution dilution to less than 10 %. More details about the unit have been published previously [26].

#### 2.1.2. Pilot unit

A pilot system was built to assess long-term performance of different membranes (Fig. 2). Similar to the bench scale unit, the pilot had closed



**Table 1**  
Membrane properties.

Parameter	Units	Module 1		Module 2	Module 3
		A	B		
		Toyobo HPC3205	Toyobo HPC3205	Aromatec 2''	Aquaporin AQP-HFFO 2
Testing unit		Bench	Pilot	Bench & Pilot	Bench
Membrane area	m <sup>2</sup>	31.5	31.5	0.5	2.3
Material		Cellulose triacetate (CTA)	Cellulose triacetate (CTA)	Thin film composite (TFC)	Aquaporin protein
Operating mode	Feed Solution	One-Pass	One-Pass	Recirculation	One-Pass
	Draw Solution	One-Pass	One-Pass	One-Pass	One-Pass
Operating flowrate	Feed Solution	1.35	1.35	1.5	1.0
	Draw Solution	0.35	0.35	1.5	0.4
Operating pressure	Feed Solution	3	3	6	5
	Draw Solution	30	30	4.5	3
K <sub>m</sub> - Mass transfer coefficient		0.0063	0.015	0.0069	0.0286
	20 °C	N.M.	0.195	2.268	N.M.
A - Water <sup>1</sup> Permeability	25 °C	0.275	0.228	2.805	1.03
	30 °C	N.M.	0.26	3.343	N.M.
	20 °C	N.M.	0.05	0.319	N.M.
B - Solute <sup>1</sup> Permeability	25 °C	0.114	0.054	0.391	0.1
	30 °C	N.M.	0.059	0.464	N.M.
Flowrate	Feed Solution	N.M.	0.05	0.319	N.M.
	Draw Solution	N.M.	0.059	0.464	N.M.

Note 1: Module 1A and Module 2 were only operated at 25 °C in bench tests.  
N.M. Not measured.

loops for the feed and draw solution as well as sensors to monitor the main process parameters of temperature, pressure, and conductivity. Positive displacement pumps were used to circulate the water within the loops (KNF, Switzerland). Cartridge filters (5μ, Atlas Filtri, Italy) were installed before the membrane module to remove any suspended solids. A LabVIEW real-time system (cRIO 9035, National Instruments, USA) was used to control the operation of the unit, to record relevant process performance parameters, and to maintain constant flow rates based on a PID controller. Depending on the membrane operating mode, the water flux was measured either by flowmeters in the inlet and outlet of each stream (Omega, USA) or by the difference in weight in an intermediate buffer tank with a 60 Kg Balance (Mettler Toledo, Switzerland). The buffer tank was only used with module 2 since it operates in recirculation mode. This intermediate tank allows the feed solution to be concentrated to the desired recovery; it is kept constant by adding fresh feed and wasting part of the concentrated solution (batch and bleed mode). To ensure sufficient feed and draw solution could be provided for the test runs (minimum 50 h continuous operation), large 5 m<sup>3</sup> feed and draw solution tanks were installed.

### 2.1.3. Membranes

Three different commercial hollow fiber FO membranes were used during this evaluation; each representing a different chemistry and manufacturer:

- Modules 1A & 1B, cellulose triacetate (CTA); manufacturer: Toyobo,
- Module 2, polyamide thin film composite (TFC); manufacturer: Aromatec
- Module 3, aquaporin proteins [53], (AP); manufacturer: Aquaporin

Module 1 was operated in a “single-pass” mode, i.e. without any recirculation of the feed or draw solution. Tests were conducted in counter-current mode with the draw solution flowing inside the fibers while the feed solution flows on the outside, as specified by the manufacturer [54].

Module 2, due to its lower membrane area, was operated with feed recirculation, while the draw solution was in single-pass. The module was operated in counter-current mode with the feed solution flowing inside the fiber and draw solution flowing on the outside. The membrane's active layer was in contact with the feed solution [55–57]

Module 3 was operated in single-pass mode and in counter-current configuration. The feed solution was flowing inside the fibers (active layer) while the draw solution was on the outside [58,59].

More details on the membranes, including membrane properties and operating conditions are shown in Table 1. Single-pass modules are considered more efficient and desirable for full-scale implementation, but those modules were not available from Aromatec at the time of this study. Aromatec has recently developed a 4'' module that can operate in single-pass and that will be considered for future studies.

## 2.2. System operation

### 2.2.1. Operating modes

Module 1 was tested in a “single-pass” mode, i.e. without any recirculation of the feed or draw solution. Tests were conducted in counter-current mode with the draw solution inside the fibers and the feed solution on the outside, as specified by the manufacturer [54].

Due to its lower membrane area and lower flux, the feed for Module 2 recirculated while the draw solution was in single-pass mode. The module was also operated in counter-current mode but with the feed solution inside the fiber and draw solution on the outside, opposite to Module 1. The membrane's active layer was in contact with the feed solution [2,55,56].

Module 3 was operated in single-pass mode and in counter-current configuration like Module 2, i.e. feed solution inside the fibers and the draw solution on the outside.

### 2.2.2. Baseline tests

Baseline tests for membrane screening were conducted using tap water as feed solution (90 mg/L TDS) pretreated with activated carbon (Atlas Filtri, Italy) to remove chlorine. The draw solution was 58,500 mg/L (1 M) NaCl prepared using tap water also pretreated with activated carbon.

### 2.2.3. Benchmark tests

Benchmark performance tests were conducted to assess membrane performance stability before and after each test with industrial wastewater. These tests are conducted as a reference to determine if fouling and/or membrane damage have occurred due to operation with real wastewater. Synthetic NaCl feed solution (2500 mg/L - mimicking the

**Table 2**  
Chemical composition of industrial wastewater.

Parameters	Units	Measurement
pH	–	7.55
Conductivity	uS/cm	2532
Turbidity	NTU	0.46
Apparent total dissolved solids (TDS)	mg/L	1727
Chlorine	mg/L	0.05
Inorganic carbon (IC)	mg/L	58.8
Total organic carbon (TOC)	mg/L	11.9
Total nitrogen (TN)	mg/L	5.2
Chloride	mg/L	497
Sulfate	mg/L	521
Sodium	mg/L	621
Magnesium	mg/L	27.9
Calcium	mg/L	20.6

TDS of the industrial process water) and synthetic seawater (40,000 mg/L NaCl) were used for the benchmark reference test and both solutions were prepared using tap water pretreated with activated carbon (Atlas Filtri, Italy).

### 2.3. Water quality and analysis

#### 2.3.1. Feed solution: wastewater from the oil and gas industry

The wastewater was a combination of different process wastewater streams from natural gas processing facilities in Qatar [15,60]. Pre-treatment included a membrane bioreactor for soluble organics and suspended solids removal. Since this is an industrial wastewater, compositional changes have been observed over time (based on the plant operation); Table 2 shows the feed water composition of the wastewater used during the evaluation.

#### 2.3.2. Draw solution: synthetic seawater

A synthetic 40,000 mg/L NaCl solution, within the expected salinity of the Arabian Gulf seawater (which ranges from 34 to 48 g/L) [61,62], was prepared using dechlorinated tap water. Synthetic seawater was used instead of real seawater to assess the impact of the real wastewater on the membrane without any possible interference by organics in the seawater.

#### 2.3.3. Laboratory analyses

The ionic composition of both solutions was analyzed by ion chromatography (ICS 6000, Thermoscientific, USA). Metals were analyzed by inductively coupled plasma (ICAP 6500, Thermoscientific, USA). Chlorine analyses were conducted using Hach method 8021 (DR 5000, Hach, USA). Organic and inorganic carbon analyses and total nitrogen analysis were performed based on the combustion method (TOC-V, Shimadzu, Japan). The organics were further characterized as hydrophilic/hydrophobic using a liquid chromatography system coupled with an organic carbon detector (Suez M9 SEC, Paris, France) and a Toyo-Pearl column resin (Tosoh Bioscience, Japan) for separation [63].

### 3. Modeling

There are many performance-predictive models in the literature [19, 37,42–49] capable of predicting water flux and reverse solute flux (RSF) of small membrane modules since the concentration profile inside the module does not change significantly. However, for larger modules, the feed and draw solution concentrations change as the solutions flow through the module. None of available models predicted feed and draw solution outlet concentrations/flows and the expected feed recovery and draw solution dilution under different operating conditions. Additionally, none of them developed the flux profile along the length of the module, another feature that can provide insights on module performance. Other non-publicly available models focused on full scale system design and optimization rather than individual commercial module

performance [50–52]. To assess the performance of the commercial OC membrane modules, a performance model was developed to address the limitations mentioned above. Fig. S1 shows the user interface.

The water flux is calculated based on Eqs. 1 and 2 with the active layer facing the feed and draw solutions respectively [19].

$$J_w = K_m \ln \left( \frac{A \Pi_{draw} + B}{A \Pi_{feed} + J_v + B} \right) (AL - \text{facing feed solution}) \quad (1)$$

$$J_w = K_m \ln \left( \frac{A \Pi_{draw} - J_v + B}{A \Pi_{feed} + B} \right) (AL - \text{facing draw solution}) \quad (2)$$

where  $J_w$  is the water flux,  $K_m$  is the mass transfer coefficient,  $A$  is the membrane water permeability,  $B$  is the salt permeability, and  $\Pi_{feed}$  and  $\Pi_{draw}$  are the osmotic pressures for the feed and draw solutions respectively.

The solute flux is calculated based on Eq 3 [19]

$$J_s = \frac{B}{A \beta R_g T} J_w \quad (3)$$

where  $J_s$  is the membrane solute flux,  $\beta$  is the van't Hoff coefficient,  $R_g$  is the universal gas constant and  $T$  is the absolute temperature.

Since the commercial modules have large membrane areas, the properties of the feed and draw solutions change as the solutions pass through the module. To account for those variations, the membrane was divided into discrete small sections ( $\Delta m$ ) and the modeling equations were applied in each section, yielding a flux profile across the module (Figs. 3, 4).

The model is capable of predicting the performance of both co-current and counter-current configurations. For co-current flow, a mass balance is performed in each section  $\Delta m$ ; the model calculates the water and solutes fluxes of each section, based on Eq. 1,2 and 3, and then calculates the flows and concentrations leaving each section, using Eq. 4,5,6 and 7.

$$FF_{i+1} = FF_i - J_{wi} \Delta m \quad (4)$$

$$DF_{i+1} = DF_i + J_{wi} \Delta m \quad (5)$$

$$FC_{i+1} = \frac{FC_i FF_i + J_{si} \Delta m}{FF_{i+1}} \quad (6)$$

$$DC_{i+1} = \frac{DC_i DF_i - J_{si} \Delta m}{DF_{i+1}} \quad (7)$$

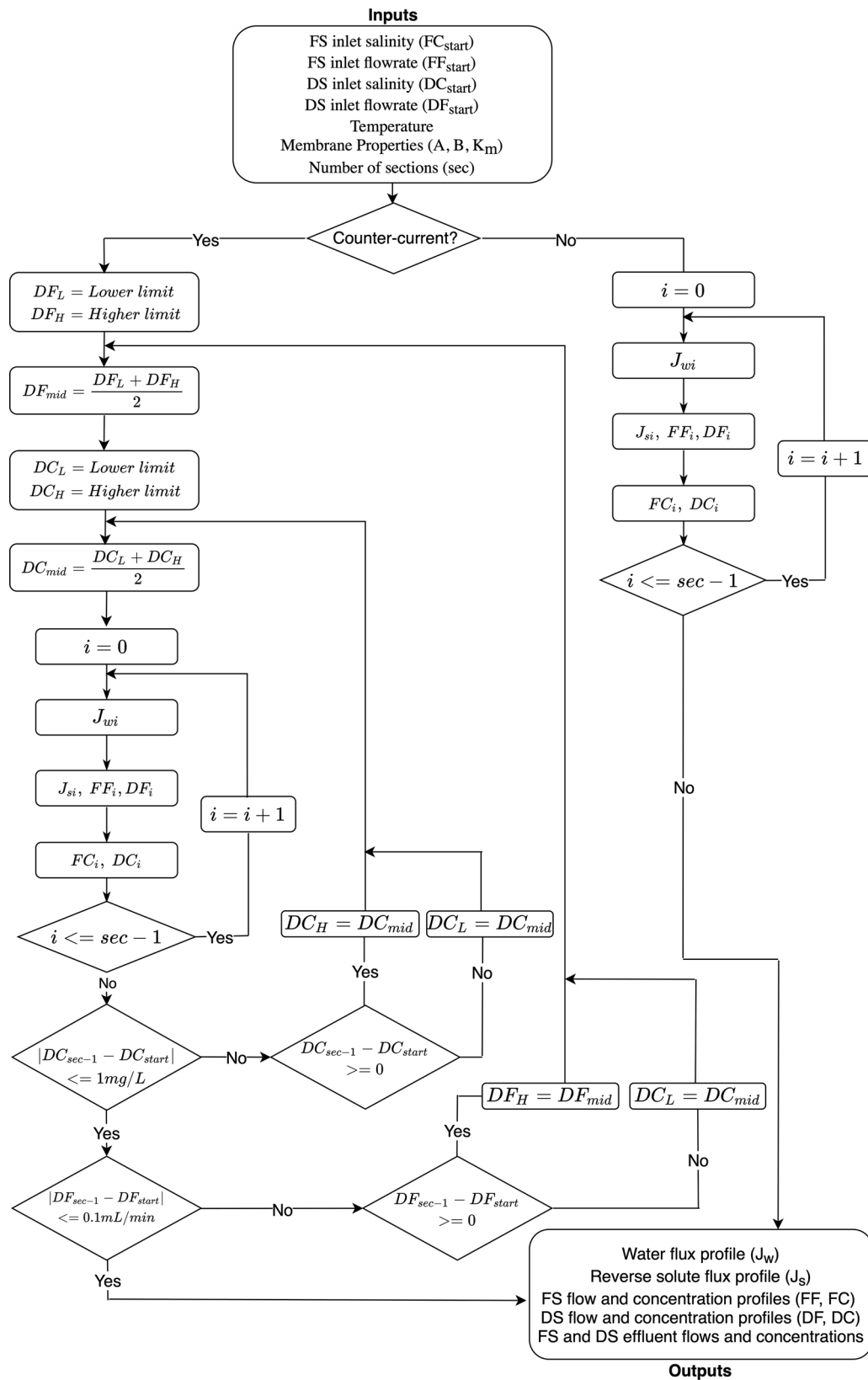
where  $FF$  and  $DF$  are the feed and draw flow in each section respectively and  $FC$  and  $DC$  are the feed and draw concentrations for each section respectively.

For counter-current mode, an iterative process is implemented to determine the correct outputs. The feed and draw solution flows and concentrations are entered as inputs and based on those, the model estimates the feed & draw solution outputs (flow and concentration) assuming co-current operation mode. Then it calculates the water and solute fluxes for each section based on Eqs. 1,2 and 3, and the feed and draw solution flows and concentrations, based on Eq. 4,6,8 and 9. The model compares those with the draw solution initial input values. If they do not match, new draw solutions outlet values are calculated using root finding methods, and the process iterates again until the final values match the draw solution inputs with a tolerance of 1 mg/L for the concentration and 0.1 mL/min for the flow rate as seen in Fig. 3.

$$DF_{i+1} = DF_i - J_{wi} \Delta m \quad (8)$$

$$DC_{i+1} = \frac{DC_i DF_i + J_{si} \Delta m}{DF_{i+1}} \quad (9)$$

For the calculation of osmotic pressure and diffusivities, the model assumes NaCl solutions. The osmotic pressure is calculated based on Eq.



10 [64]:

$$\Pi = -\phi \frac{RT}{V_m} \ln(X_m) \quad (10)$$

Where  $\Pi$  is the osmotic pressure,  $\phi$  is the osmotic coefficient,  $V_m$  is the volume of water per mole (also known as partial molar volume),  $X_m$  is the mole fraction of water. The osmotic coefficient ( $\phi$ ) and water density (for the mole fraction determinations) are calculated using linear

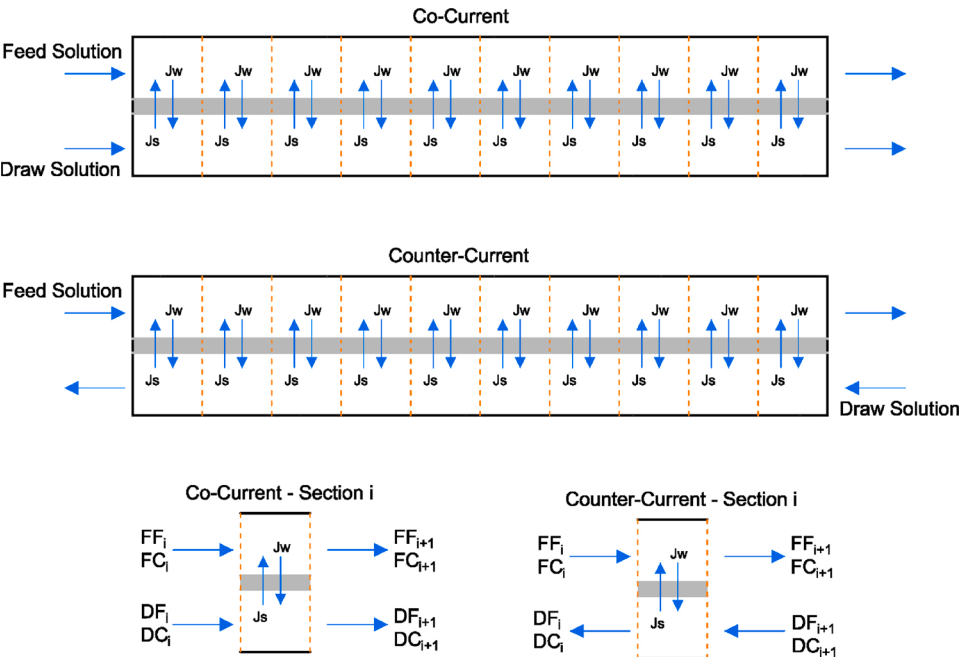


Fig. 4. Membrane sections for co-current and counter-current configurations.

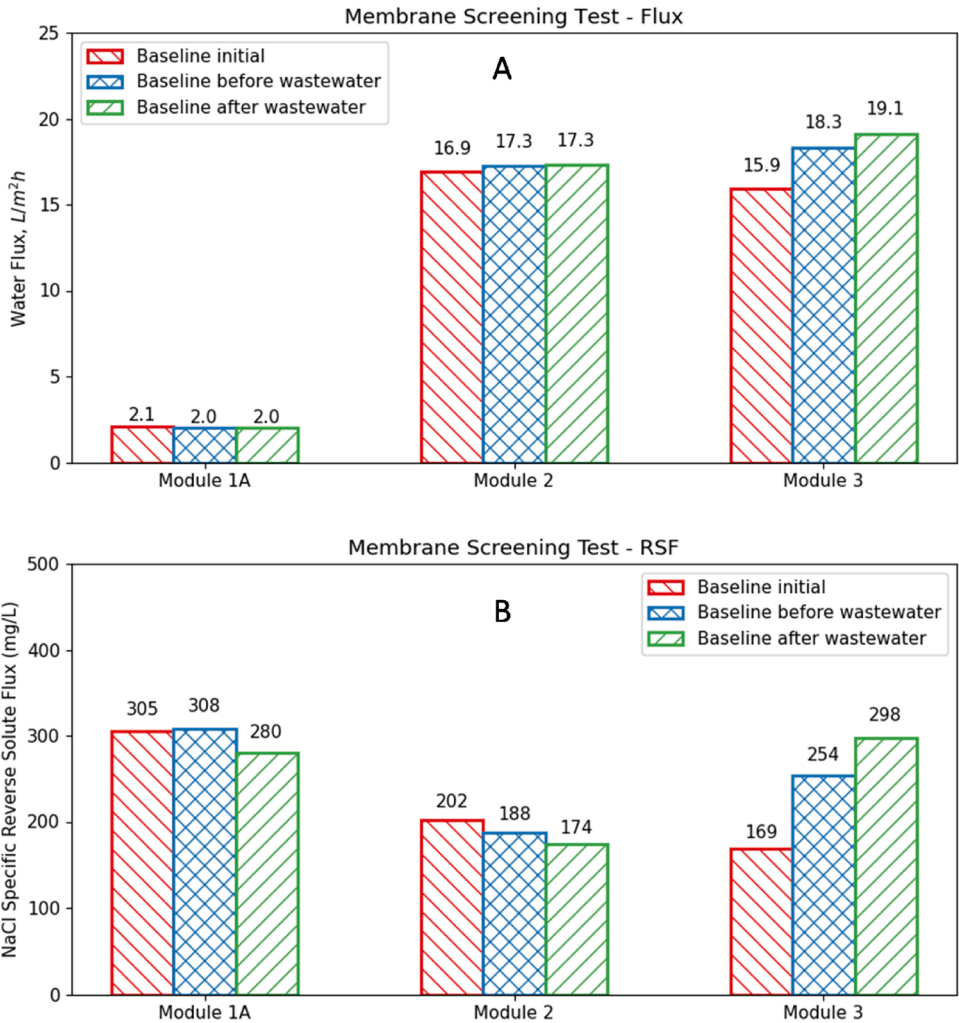


Fig. 5. Baseline performance for three different hollow-fiber FO membranes. A) Water flux, B) Specific reverse solute flux.



interpolation based on the data provided by Pitzer et al. [65].

NaCl diffusivities are calculated based on the Stokes-Einstein equation [66]

$$D = \frac{K_B T}{6\pi\eta r} \quad (11)$$

where  $D$  is the diffusivity of NaCl,  $K_B$  is the Boltzmann's constant,  $\eta$  is the dynamic viscosity and  $r$  is the Stokes radius (0.16 nm for NaCl [67]). The dynamic viscosity is calculated based on the correlation presented by Ozbek et al. [68].

As in all fitting models, the mass transfer coefficient ( $K_m$ ) and structural parameter ( $S$ ) need to be fitted based on the membrane A and B parameters and a known flux value. The fitting of the model is also performed with the same iteration process to ensure accuracy of the predictions and to account for the hydrodynamic conditions of the module. The correlation between the mass transfer coefficient ( $K_m$ ) and structural parameter ( $S$ ) is shown in Eq. 12 [56].

$$K_m = \frac{\varepsilon \cdot D}{\tau \cdot l} = \frac{D}{S} \quad (12)$$

The model also considered the effect of temperature on performance by entering A and B as a function of temperature and the model assumes the same temperature for both feed and draw solutions. The installer and executable files for the model are available in Mendeley Data: <https://doi.org/10.17632/f4w9mr5z3t> and in Github: [https://github.com/globawsc/FQ\\_Model/releases/tag/1.0](https://github.com/globawsc/FQ_Model/releases/tag/1.0)

## 4. Results and discussion

### 4.1. Membrane screening tests

Pilot testing is a key step in assessing the feasibility of OC for volume reduction of process water from gas processing facilities. However, before pilot testing, appropriate OC membranes must be chosen and their operating parameters optimized. These variables are better studied in a bench scale system since it allows wider range of conditions to be evaluated in a shorter amount of time compared to pilot testing.

For membrane selection, three commercial hollow fiber membranes were tested to compare their performance based on water flux, specific reverse salt flux, specific forward organic flux and flux stability (Fig. 5). Two baseline tests (pretreated tap water as FS and 58,500 mg/L NaCl as DS) were performed before processing industrial wastewater to check that the module performance was reproducible and stable; and to confirm that there were no significant experimental errors or variabilities between the two baselines. A 3rd baseline test was performed afterwards to assess fouling propensity and/or membrane damage. Module 2 showed a reproducible (<5%) and stable baseline performance and the highest flux of  $\approx 17 \text{ L/m}^2\text{-h}$ . Module 2 also had the lowest specific RSF of  $\approx 185 \text{ mg/L}$ , consistent with the expectations for TFC membranes. Module 1 also had a reproducible (<5%) and stable baseline results but at a much lower flux of only  $\approx 2 \text{ L/m}^2\text{-h}$  and specific RSF of  $\approx 300 \text{ mg/L}$ . Module 3 showed both an increasing baseline flux (from  $\approx 16$  to  $\approx 19 \text{ L/m}^2\text{-h}$ ), and an increasing specific RSF (170–300 mg/L), both indications that membrane damage may have occurred. Module 3's increasing flux and specific RSF could be attributed to damage on the membrane active layer (aquaporin protein) possibly due to residual chlorine that could not be removed by the activated carbon filter used to pretreat the baseline feed water [69]. Damage may have occurred even though the residual total chlorine was  $<0.04 \text{ mg/L}$  for every test conducted. This increase in flux and specific RSF could also be attributed to a broken fiber. On the basis of these results, Modules 1 & 2 were selected for subsequent pilot tests.

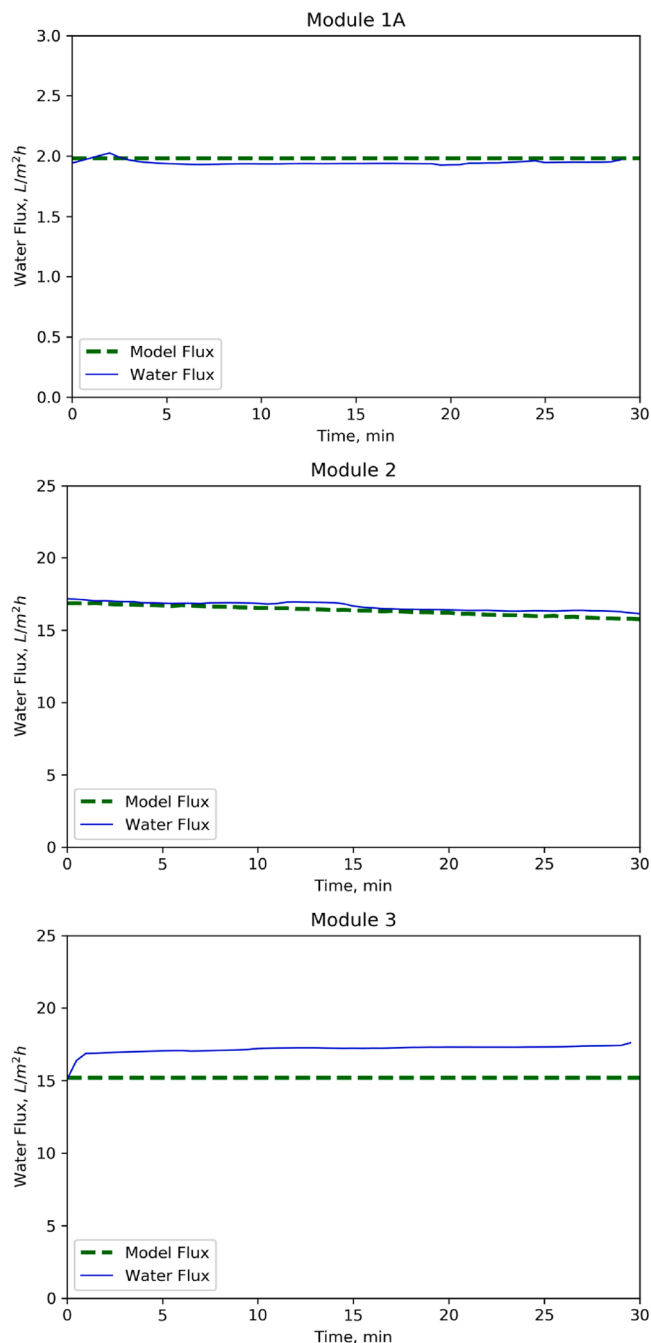


**Fig. 6.** Water flux experimental results and model prediction using real wastewater as feed solution. Counter-current vs co-current flows

### 4.2. Model results

In a model, the impact of varying critical operating conditions on process performance can be more easily assessed than through physical tests. Examples of critical parameters include the feed and draw solution flowrates and their roles in module dynamics. Higher flowrates typically translate into higher fluxes because of improved boundary layer mass transfer. However, the higher flows are usually limited by the pressure drops along the length of the module. Flowrates also impact concentration factors in systems operating in a “one-pass” configuration. To establish the optimum operating conditions for pilot studies, a model based on bench test results was developed.

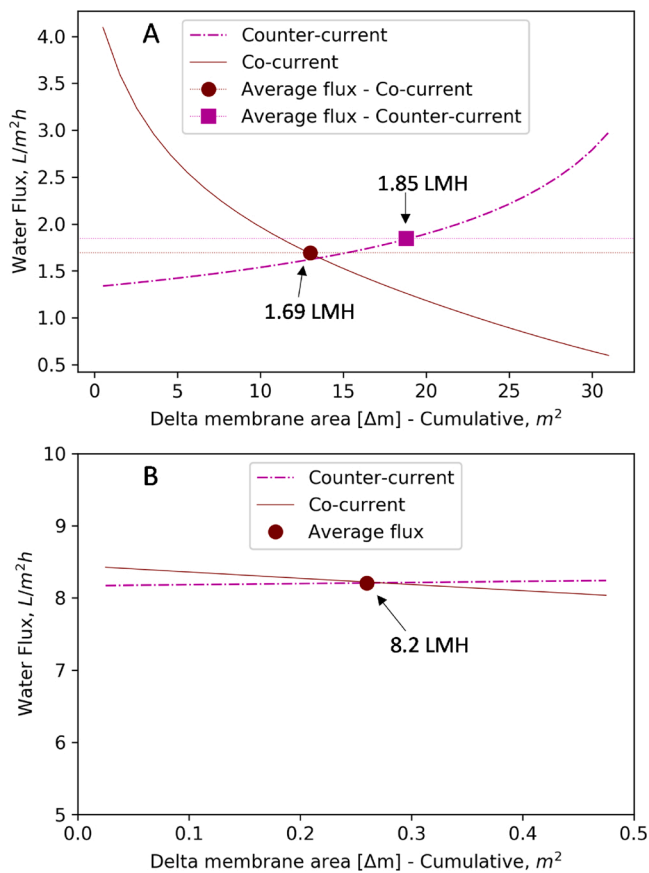


Fig. 7. Flux comparison at 75 % recovery: Counter-current vs Co-current; A) Module 1; B) Module 2.

#### 4.2.1. Operating mode

For single-pass operation with Module 1, the model was run at various feed and draw solution flowrates, feed concentration factors (CF) and draw solution dilution factors to assess their impact on performance. For Module 2 which was operated with feed recirculation, both flowrates were kept constant at 1.5 L/min, as recommended by the manufacturer. The feed concentration was increased from 2000 mg/L to 8000 mg/L to simulate a 4x concentration factor. A similar approach was implemented to simulate other concentration factors. Feed limited conditions were considered during the evaluation and presented in the SI (Fig. S2 and S3).

The performance of the model was compared with the experimental data obtained during the bench tests using industrial wastewater as feed (Fig. 6). The A and B parameters for each membrane were determined by conducting RO experiments and measuring the water permeability and rejection. For modules 1A and 2, the model prediction matched the experimental data with less than 2 % deviation. Module 3, however, had 20 % higher flux compared to the expected value based on the theoretical model. It is possible that some of the constituents in the real wastewater could have affected the membrane performance since the water flux over time showed an increasing trend, as seen in Fig. 6C. Since Module 3 is based on aquaporin proteins, it is more sensitive to the water composition and it may be better suited to treat different types of water like those in the food industry [58,70].

The model reveals very different flux profiles depending on the mode of operation. For Module 1, co-current operation produced an exponential flux decline while counter-current operation resulted in an exponential flux increase across the length of the module. This is related to the changes in the concentration gradients due to the changes in the feed and draw solution salinities. At a CF of 4, counter-current operation is more efficient since the average water flux is slightly higher at 1.85 vs

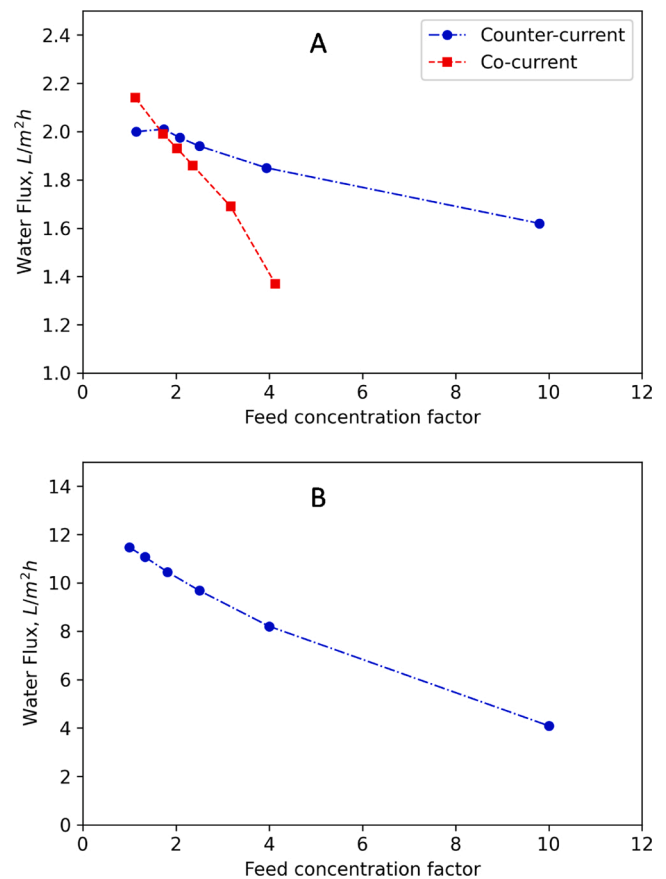


Fig. 8. Simulated water flux as function of feed concentration factor. A) Module 1; B) Module 2.

1.69 L/m<sup>2</sup>·h (Fig. 7A).

For Module 2, both operating modes yielded similar results with an average flux of 8.2 L/m<sup>2</sup>·h (Fig. 7B). The model does not show significant differences between co-current and counter-current due to the small membrane area (0.5 m<sup>2</sup>), high flowrates (1.5 L/min) and the limited impact of permeation on feed concentration along the module's length. For consistency with Module 1, all the experiments with Module 2 were conducted in counter-current mode.

#### 4.2.2. Feed concentration factor

For Module 1, the flux decreased as the concentration factor increased. This is due to the decrease in the osmotic driving force across the module due to water permeation from the feed to the DS. At feed CFs > 1.7x, counter-current operation yields fluxes higher than co-current mode (Fig. 8A). In contrast, at feed CFs < 1.7x, co-current operation yields higher fluxes due to the limited changes in solution composition under these conditions. For pilot tests, counter-current operation with a CF of 4 was selected.

For Module 2, the model prediction also showed a flux decline as the CF increased (Fig. 8B). Similar to the single-pass module, the flux declined at faster rates as concentration factor increased. As with Module 1, for this module, a CF of 4 was selected for pilot testing.

#### 4.2.3. Pilot test operating conditions

Based on the model results, counter-current operation, a feed CF of 4 and a draw solution dilution factor of 4 were selected for pilot studies. At higher CFs, the decrease in osmotic pressure differential significantly reduced flux and negatively impacted performance. (SI Fig. S4). For Module 1, to operate within manufacturer's guidelines and a CF of 4 at 25 °C, a feed flowrate of 1.35 L/min and a DS flowrate of 0.35 L/min were selected. Module 2 was operated in recirculation mode, with the

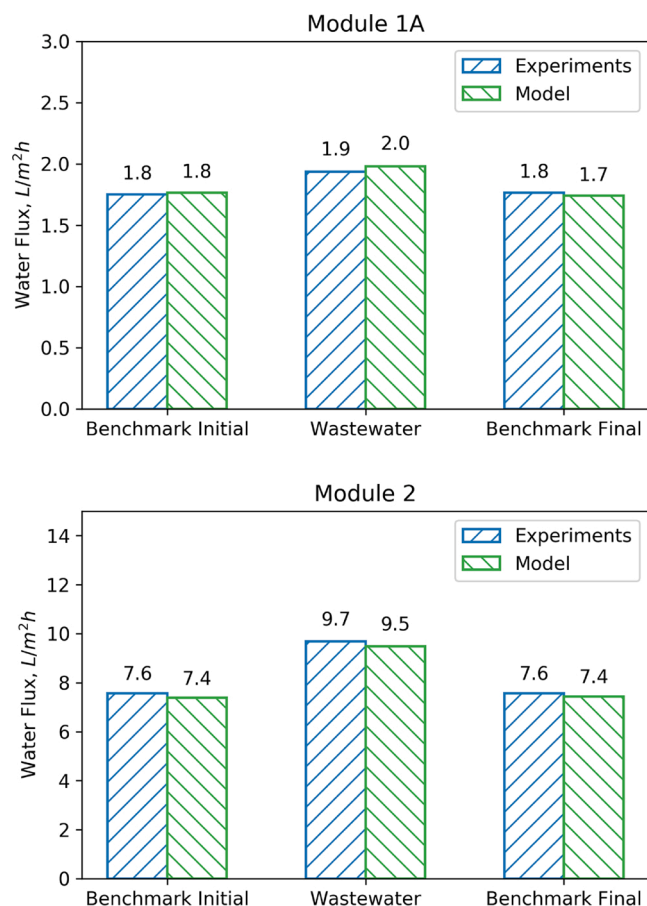


Fig. 9. Membrane water flux during bench scale tests: Experimental data vs model predictions.

feed and DS flowrates set at 1.5 L/min as recommended by the manufacturer. A feed CF of 4 was selected to ensure an accurate comparison could be made with Module 1.

#### 4.3. Bench scale test results

Bench scale experiments, under temperature control, and using both synthetic and real wastewaters were conducted to assess Module 1 & 2 performance. Each module was operated according to manufacturer recommendations until a  $4\times$  CF was achieved. Before the test, the salt precipitation potential was evaluated using OLI, a water chemistry simulation software (OLI Systems, New Jersey, USA). Based on the simulation output, no solids were formed below a  $20\times$  CF.

##### 4.3.1. Water flux

Benchmark experimental results showed that Module 2 has  $\approx 4\times$  higher flux compared to Module 1. This is in agreement with previous studies showing that TFC membranes have higher water permeability compared to CTA due to different chemistry properties [56,71,72]. Also, the flux obtained experimentally was within 5 % the model predictions (Fig. 9).

To give a better indication of performance in service, industrial wastewater was used as feed. Experimental results for both modules showed stable performance and the model flux predictions matched the experimental data indicating that no fouling had occurred. On wastewater, Module 2 had a  $5\times$  higher flux than Module 1 (9.7 vs. 1.9 L/m<sup>2</sup>·h). The 25 % increase compared with benchmark flux was due to the lower salinity of the wastewater (2500 mg/L TDS for the benchmark (osmotic pressure of 2 bars) vs 1700 mg/L TDS for the real wastewater (osmotic pressure of 1.3 bars)). Additionally, benchmark tests were conducted

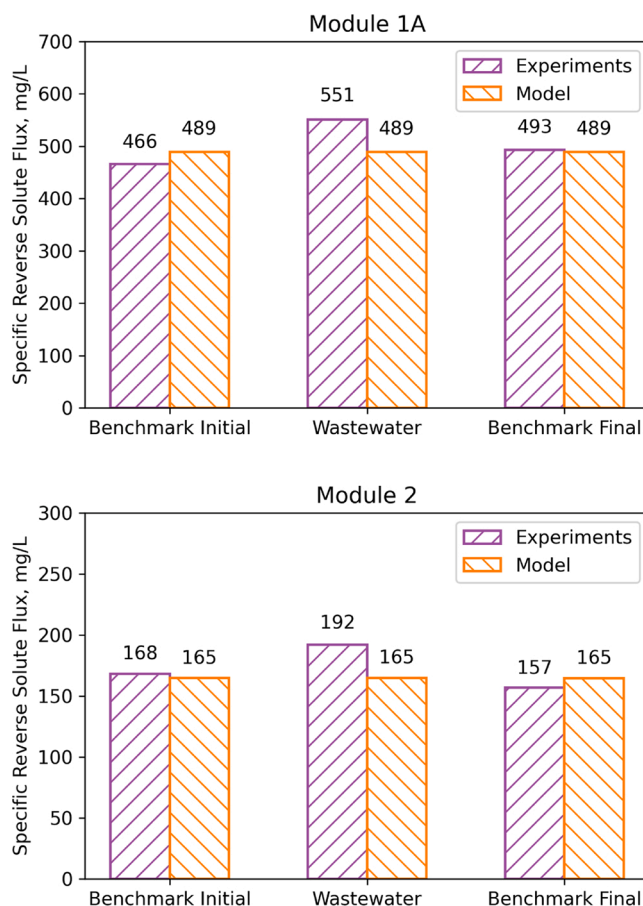


Fig. 10. Membrane specific reverse solute flux during bench scale tests: Experimental data vs. model predictions.

both before and after the real wastewater tests and results were similar, and matched the model predicted values within 3% accuracy, supporting the conclusion that no significant fouling had occurred. However, longer term pilot tests are deemed necessary to confirm long-term fouling propensities.

##### 4.3.2. Specific reverse solute flux and organic rejection

Experimental results showed that Module 2 has  $3\times$  lower specific RSF compared to Module 1 (Fig. 10), consistent with the superior rejection typically observed with TFC membranes. Other studies have shown significantly lower RSF on TFC membranes compared to CTA due to the differences in permeability and diffusivity [25,56,71]. CTA membranes are made of a polyester fabric embedded in a support layer. Those membranes have a typical salt rejection between 85–94% [73]. On the other hand, TFC membranes are made via interfacial polymerization with a polyamide active layer. These membranes have a typical rejection of 96–99 % [74].

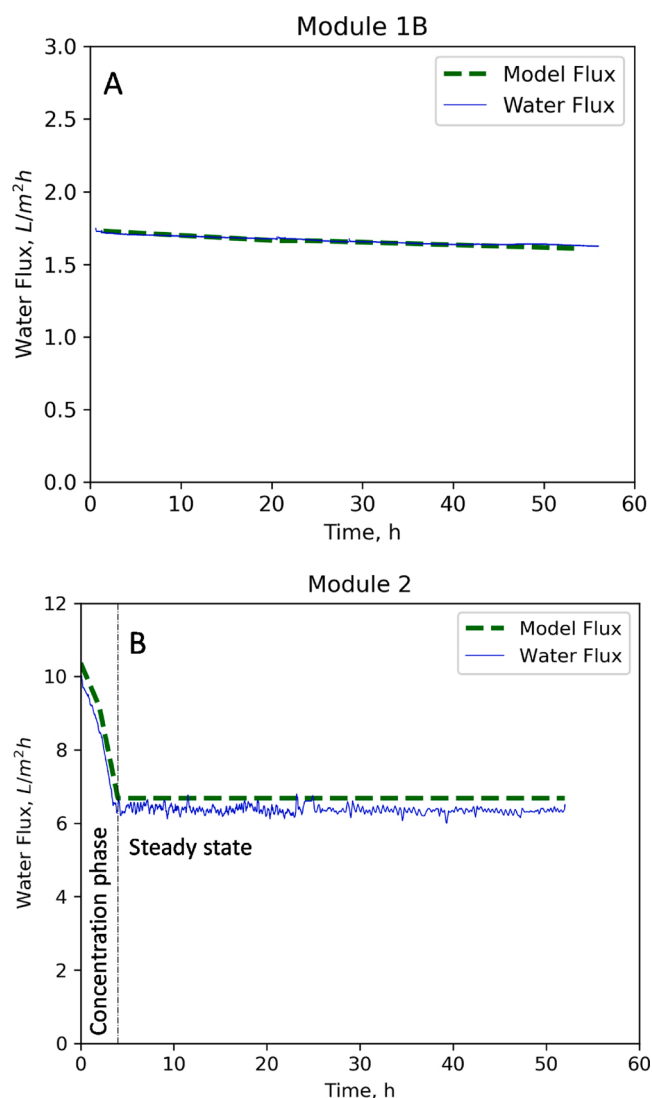
In this study, the CTA membranes (Modules 1A and 1B) evaluated had a water permeability (at 25C) of 0.2–0.3 LMH/bar while TFC membrane had a permeability of 2.5–3 LMH/bar; almost 10X higher; hence the TFC membrane (module 2) is expected to have higher water flux. In terms of rejection, the CTA membrane has a salt permeability coefficient of approximately 0.1 LMH while the TFC module as a salt permeability of approximately 0.4 LMH. Even though the TFC module has a higher salt permeability (4X higher compared to CTA); their salt rejection is better due to the higher water permeability (10X).

The RSF model predictions for the real wastewater were slightly lower than the measured values. One hypothesis is that this could be attributed to the other ions in the wastewater which may have different diffusivities [50,75]; the model only considered sodium chloride.

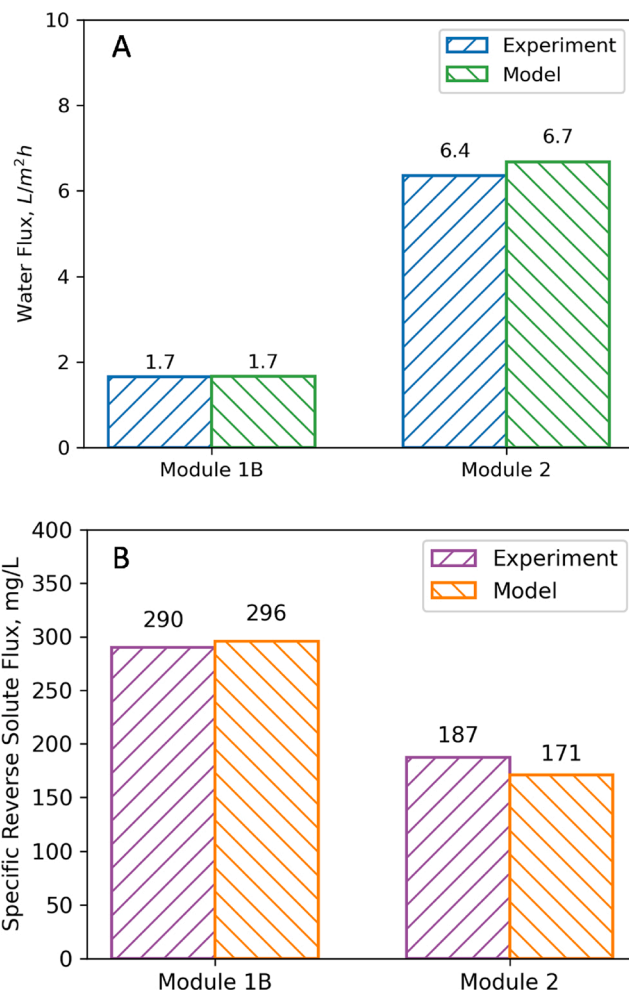
**Table 3**

Ion rejection for experiments conducted with industrial wastewater.

Parameters	Rejection*	
	Module 1A	Module 2
Chloride	86 %	87 %
Sodium	90 %	93 %
Potassium	–	90 %
Sulfate	97 %	>99 %
Magnesium	82 %	>99 %
Calcium	–	>99 %
Total organic carbon (TOC)	>99 %	>99 %
Total nitrogen (TN)	>99 %	>99 %

**Fig. 11.** Pilot benchmark flux profile: Experimental vs Model.

The specific forward organic solute flux from the wastewater to the seawater was  $<0.5$  mg TOC/L of permeate for both modules, indicating excellent rejection of these organics by both TFC and CTA membranes. For full-scale implementation, this is a critical parameter as it shows that insignificant amounts of organics from the feed are discharged in the seawater returned to the ocean. The feed and DS were also analyzed using liquid chromatography with an organic carbon detector (LC–OCD) [63] and results showed that most of the organics in the feed solution are hydrophilic, and thus they would likely remain in solution rather than being adsorbed into the membrane surface [76].

**Fig. 12.** Pilot benchmark test: Comparison between Module 1B and Module 2. A) Water flux. B) Specific RSF.

A feed solution mass balance showed no loss of organic carbon, supporting the high rejection of the TOC by the membranes and reinforcing the low fouling potential of the industrial wastewater. The rejection of individual ions, TOC and total nitrogen for Modules 1 & 2 are compared in Table 3.

#### 4.4. Pilot study – extended benchmark test

To verify the long-term membrane performance, a 50 h long extended benchmark test was conducted using the pilot system as described in section 2. For the TFC chemistry, a new HP3205 module (Module 1B) was used for the CTA chemistry, while the Module 2 from earlier bench tests was used. Both modules showed stable performance profiles (Fig. 11). Both modules also showed flux results comparable with the bench scale data and matched model predictions within 5 % accuracy (Fig. 12 A). Module 2 has  $\approx 4\times$  higher flux compared to Module 1B. Regarding specific RSF, Module 2 has lower salt permeability compared to Module 1 (Fig. 12B); however, the specific RSF obtained in the pilot unit for Module 1B was lower than the value obtained with Module 1A in the bench scale evaluation. The reason for this is the different salt permeability coefficient (B) between the two modules. For modules 1A and 1B the salt permeability values were 0.114 and 0.054 L/m<sup>2</sup>·h respectively (Table 1). Those differences may be attributed to the membrane manufacturing process. When the appropriate A and B parameters for each module are input into the model, the predictions matched the experimental data predictions within  $\pm 2$ –5 % for the water flux and  $\pm 5$ –10 % for the RSF. Pilot testing is in progress to assess the



long-term impact of the industrial wastewater on both membranes.

## 5. Conclusions

Three commercial hollow-fiber FO membranes (CTA, TFC, aquaporin proteins) were screened to assess their performance in reducing the volume of wastewater generated during natural gas processing.

The main outcomes of the of the project are:

- A mathematical model capable of predicting membrane performance, including flow and concentration profiles across the module, was developed. Based on the model output, bench scale operating conditions were defined to assess process performance in full-scale applications. Model predictions showed that:
  - o Counter-current operation provides higher average water flux and feed higher concentration factors compared to co-current operation.
  - o A feed concentration factor of 4x appears to be the optimum for this application since at higher concentration factors, the driving force across the module decreases significantly, negatively impacting performance.
- Results with industrial wastewater showed that the TFC chemistry (Module 2) had a  $\approx 5$ x higher water flux (9.7 vs. 1.9 L/m<sup>2</sup>-h) and  $\approx 3$ x lower specific reverse solute flux (192 vs 551 mg/L) when compared to CTA chemistry (Module 1).
- Both TFC & CTA membrane chemistries showed <5% fouling at the optimized operating conditions.
- Water quality data revealed high organic rejection for both membranes, with a specific forward organic solute flux of <0.5 mg/L, indicating that the flow of organics into the desalination plant brine would not result in significant environmental impact.
- Pilot unit performance over 50 h of operation was comparable with the bench scale data and matched model predictions typically within 2–5 % for the water flux and 5–10 % for the RSF.

## Declaration of Competing Interest

The authors declare that they have no known competing financial interests or personal relationships that could have appeared to influence the work reported in this paper.

## Acknowledgments

This work was made possible by National Priorities Research Programme (NPRP) grant NPRP 10-0118-170191 from the Qatar National Research Fund Grant ID: NPRP 10-0118-170191 (a member of Qatar Foundation). The findings achieved herein are solely the responsibility of the authors and do not necessarily represent the official views of ConocoPhillips or the Qatar National Research Fund.

The research team would like to acknowledge their colleagues at the ConocoPhillips Global Water Sustainability Centre including: Altaf Hussain, Nabin Upadhyay, Eman AlShamari for their support with the bench scale testing and lab analyses.

The author also would like to thank Abdelrahman Awad, Reem Jalab and Dan Cortes from Qatar University for their support with the pilot evaluation.

## Appendix A. Supplementary data

Supplementary material related to this article can be found, in the online version, at doi:<https://doi.org/10.1016/j.jwpe.2020.101760>.

## References

- [1] A. Fakhru'l-Razi, A. Pendashteh, L.C. Abdullah, D.R.A. Biak, S.S. Madaeni, Z. Z. Abidin, Review of technologies for oil and gas produced water treatment, *J. Hazard. Mater.* 170 (2009) 530–551, <https://doi.org/10.1016/j.jhazmat.2009.05.044>.

- [2] S. Zhao, J. Minier-Matar, S. Chou, R. Wang, A.G. Fane, S. Adham, Gas field produced/process water treatment using forward osmosis hollow fiber membrane: membrane fouling and chemical cleaning, *Desalination*. 402 (2017) 143–151, <https://doi.org/10.1016/j.desal.2016.10.006>.
- [3] A. Hassan, Review of the global oil and gas industry: a concise journey from ancient time to modern world, *Pet. Technol. Dev. J.* 3 (2014) 20.
- [4] S. Adham, A. Hussain, J. Minier-Matar, A. Janson, R. Sharma, Membrane applications and opportunities for water management in the oil & gas industry, *Desalination*. (2018), <https://doi.org/10.1016/j.desal.2018.01.030>.
- [5] R. Does, A. Hussain, M. Katebah, S.S. Adham, Using advanced water treatment technologies to treat produced water from the petroleum industry, *SPE Int. Prod. Oper. Conf. Exhib.* (2012), <https://doi.org/10.2118/157108-MS>.
- [6] P. Xu, J.E. Drewes, Viability of nanofiltration and ultra-low pressure reverse osmosis membranes for multi-beneficial use of methane produced water, *Sep. Purif. Technol.* 52 (2006) 67–76, <https://doi.org/10.1016/j.seppur.2006.03.019>.
- [7] D.L. Shaffer, L.H. Arias Chavez, M. Ben-Sasson, S. Romero-Vargas Castrillón, N. Y. Yip, M. Elimelech, Desalination and reuse of high-salinity shale gas produced water: drivers, technologies, and future directions, *Environ. Sci. Technol.* 47 (2013) 9569–9583, <https://doi.org/10.1021/es401966e>.
- [8] B.D. Coday, N. Almaraz, T.Y. Cath, Forward osmosis desalination of oil and gas wastewater: impacts of membrane selection and operating conditions on process performance, *J. Memb. Sci.* 488 (2015) 40–55, <https://doi.org/10.1016/j.memsci.2015.03.059>.
- [9] W. Pronk, A. Ding, E. Morgenroth, N. Derlon, P. Desmond, M. Burkhardt, B. Wu, A. G. Fane, Gravity-driven membrane filtration for water and wastewater treatment: a review, *Water Res.* 149 (2019) 553–565, <https://doi.org/10.1016/j.watres.2018.11.062>.
- [10] B.D. Coday, P. Xu, E.G. Beaudry, J. Herron, K. Lampi, N.T. Hancock, T.Y. Cath, The sweet spot of forward osmosis: treatment of produced water, drilling wastewater, and other complex and difficult liquid streams, *Desalination* 333 (2014) 23–35, <https://doi.org/10.1016/j.desal.2013.11.014>.
- [11] A. Janson, A. Santos, M. Katebah, A. Hussain, J. Minier-Matar, S. Judd, S. Adham, Assessing the biotreatability of produced water from a Qatari gas field, *SPE J.* 20 (2014).
- [12] R. Jalab, A.M. Awad, M.S. Nasser, J. Minier-Matar, S. Adham, S.J. Judd, An empirical determination of the whole-life cost of FO-based open-loop wastewater reclamation technologies, *Water Res.* 163 (2019), 114879, <https://doi.org/10.1016/j.watres.2019.114879>.
- [13] B. Xiong, A.L. Zydney, M. Kumar, Fouling of microfiltration membranes by flowback and produced waters from the Marcellus shale gas play, *Water Res.* 99 (2016) 162–170.
- [14] R. Valladares Linares, Z. Li, V. Yangali-Quintanilla, N. Ghaffour, G. Amy, T. Leiknes, J.S. Vrouwenvelder, Life cycle cost of a hybrid forward osmosis - low pressure reverse osmosis system for seawater desalination and wastewater recovery, *Water Res.* 88 (2016) 225–234, <https://doi.org/10.1016/j.watres.2015.10.017>.
- [15] J.M. Sheikhan, I. Zainab, A. Janson, S. Adham, Others, qatargas wastewater treatment plants: an advanced design for water reuse, *Int. Pet. Technol. Conf.* (2015).
- [16] L.D. Nghiem, T. Ren, N. Aziz, I. Porter, G. Regmi, Treatment of coal seam gas produced water for beneficial use in Australia: a review of best practices, *Desalin. Water Treat.* 32 (2011) 316–323.
- [17] K. Farahbakhsh, S.S. Adham, D.W. Smith, Monitoring the Integrity of low-pressure membranes, *J. American Water Work. Assoc.* 95 (2003) 95–107.
- [18] M. Kumar, S. Adham, J. DeCarolis, Reverse osmosis integrity monitoring, *Desalination*. 214 (2007) 138–149.
- [19] C.Y. Tang, Q. She, W.C.L. Lay, R. Wang, A.G. Fane, Coupled effects of internal concentration polarization and fouling on flux behavior of forward osmosis membranes during humic acid filtration, *J. Memb. Sci.* 354 (2010) 123–133, <https://doi.org/10.1016/j.memsci.2010.02.059>.
- [20] B. Aftab, Y.S. Ok, J. Cho, J. Hur, Targeted removal of organic foulants in landfill leachate in forward osmosis system integrated with biochar/activated carbon treatment, *Water Res.* 160 (2019) 217–227.
- [21] W. Suwaileh, D. Johnson, D. Jones, N. Hilal, An integrated fertilizer driven forward osmosis- renewables powered membrane distillation system for brackish water desalination: a combined experimental and theoretical approach, *Desalination* 471 (2019), 114126, <https://doi.org/10.1016/j.desal.2019.114126>.
- [22] G. Amy, N. Ghaffour, Z. Li, L. Francis, R.V. Linares, T. Missimer, S. Lattemann, Membrane-based seawater desalination: present and future prospects, *Desalination* 401 (2017) 16–21, <https://doi.org/10.1016/j.desal.2016.10.002>.
- [23] W.L. Ang, A.W. Mohammad, D. Johnson, N. Hilal, Forward osmosis research trends in desalination and wastewater treatment: a review of research trends over the past decade, *J. Water Process Eng.* 31 (2019), 100886.
- [24] H. Luo, Q. Wang, T.C. Zhang, T. Tao, A. Zhou, L. Chen, X. Bie, A review on the recovery methods of draw solutes in forward osmosis, *J. Water Process Eng.* 4 (2014) 212–223.
- [25] J. Minier-Matar, A. Hussain, A. Janson, R. Wang, A.G. Fane, S. Adham, Application of forward osmosis for reducing volume of produced/Process water from oil and gas operations, *Desalination*. 376 (2015), <https://doi.org/10.1016/j.desal.2015.08.008>.
- [26] J. Minier-Matar, A. Santos, A. Hussain, A. Janson, R. Wang, A.G. Fane, S. Adham, Application of hollow fiber forward osmosis membranes for produced and process water volume reduction: an osmotic concentration process, *Environ. Sci. Technol.* 50 (2016), <https://doi.org/10.1021/acs.est.5b04801>.

- [27] L. Francis, O. Ogunbiyi, J. Saththasivam, J. Lawler, Z. Liu, A comprehensive review of forward osmosis and niche applications, *Environ. Sci. Water Res. Technol.* (2020).
- [28] R.W. Holloway, A.E. Childress, K.E. Dennett, T.Y. Cath, Forward osmosis for concentration of anaerobic digester centrate, *Water Res.* 41 (2007) 4005–4014, <https://doi.org/10.1016/j.watres.2007.05.054>.
- [29] S. Zhao, L. Zou, C.Y. Tang, D. Mulcahy, Recent developments in forward osmosis: opportunities and challenges, *J. Memb. Sci.* 396 (2012) 1–21, <https://doi.org/10.1016/j.memsci.2011.12.023>.
- [30] T.Y. Cath, A.E. Childress, M. Elimelech, Forward osmosis: principles, applications, and recent developments, *J. Memb. Sci.* 281 (2006) 70–87, <https://doi.org/10.1016/j.memsci.2006.05.048>.
- [31] L. Setiawan, R. Wang, K. Li, A.G. Fane, Fabrication of novel poly(amide-imide) forward osmosis hollow fiber membranes with a positively charged nanofiltration-like selective layer, *J. Memb. Sci.* 369 (2011) 196–205, <https://doi.org/10.1016/j.memsci.2010.11.067>.
- [32] Y. Liu, B. Mi, Combined fouling of forward osmosis membranes: Synergistic foulant interaction and direct observation of fouling layer formation, *J. Memb. Sci.* 407–408 (2012) 136–144, <https://doi.org/10.1016/j.memsci.2012.03.028>.
- [33] K. Lutcmiah, A.R.D. Verliefde, K. Roest, L.C. Rietveld, E.R. Cornelissen, Forward osmosis for application in wastewater treatment: a review, *Water Res.* 58 (2014) 179–197, <https://doi.org/10.1016/j.watres.2014.03.045>.
- [34] A. Achilli, T.Y. Cath, E.A. Marchand, A.E. Childress, The forward osmosis membrane bioreactor: a low fouling alternative to MBR processes, *Desalination* 239 (2009) 10–21, <https://doi.org/10.1016/j.desal.2008.02.022>.
- [35] J. Wei, C. Qiu, C.Y. Tang, R. Wang, A.G. Fane, Synthesis and characterization of flat-sheet thin film composite forward osmosis membranes, *J. Memb. Sci.* 372 (2011) 292–302, <https://doi.org/10.1016/j.memsci.2011.02.013>.
- [36] W. Suwaileh, N. Pathak, H. Shon, N. Hilal, Forward osmosis membranes and processes: a comprehensive review of research trends and future outlook, *Desalination* 485 (2020), 114455, <https://doi.org/10.1016/j.desal.2020.114455>.
- [37] M.A. Hafiz, A.H. Hawari, A. Altaee, A hybrid forward osmosis/reverse osmosis process for the supply of fertilizing solution from treated wastewater, *J. Water Process Eng.* 32 (2019), 100975.
- [38] A.M. Awad, R. Jalab, J. Minier-Matar, S. Adham, M.S. Nasser, S.J. Judd, The status of forward osmosis technology implementation, *Desalination* 461 (2019) 10–21, <https://doi.org/10.1016/j.desal.2019.03.013>.
- [39] W. Gai, D.L. Zhao, T.-S. Chung, Thin film nanocomposite hollow fiber membranes comprising Na<sup>+</sup>-functionalized carbon quantum dots for brackish water desalination, *Water Res.* 154 (2019) 54–61.
- [40] F. Lotfi, S. Phuntsho, T. Majeed, K. Kim, D.S. Han, A. Abdel-Wahab, H.K. Shon, Thin film composite hollow fibre forward osmosis membrane module for the desalination of brackish groundwater for fertigation, *Desalination* 364 (2015) 108–118, <https://doi.org/10.1016/j.desal.2015.01.042>.
- [41] F.E. Ahmed, R. Hashaikh, A. Diabat, N. Hilal, Mathematical and optimization modelling in desalination: state-of-the-art and future direction, *Desalination* 469 (2019), 114092, <https://doi.org/10.1016/j.desal.2019.114092>.
- [42] A. Tiraferri, N.Y. Yip, A.P. Straub, S. Romero-Vargas Castrillon, M. Elimelech, A method for the simultaneous determination of transport and structural parameters of forward osmosis membranes, *J. Memb. Sci.* 444 (2013) 523–538, <https://doi.org/10.1016/j.memsci.2013.05.023>.
- [43] Y. Xu, X. Peng, C.Y. Tang, Q.S. Fu, S. Nie, Effect of draw solution concentration and operating conditions on forward osmosis and pressure retarded osmosis performance in a spiral wound module, *J. Memb. Sci.* 348 (2010) 298–309, <https://doi.org/10.1016/j.memsci.2009.11.013>.
- [44] J.R. McCutcheon, M. Elimelech, Influence of concentrative and dilutive internal concentration polarization on flux behavior in forward osmosis, *J. Memb. Sci.* 284 (2006) 237–247, <https://doi.org/10.1016/j.memsci.2006.07.049>.
- [45] G.T. Gray, J.R. McCutcheon, M. Elimelech, Internal concentration polarization in forward osmosis: role of membrane orientation, *Desalination* 197 (2006) 1–8, <https://doi.org/10.1016/j.desal.2006.02.003>.
- [46] S. Chou, L. Shi, R. Wang, C.Y. Tang, C. Qiu, A.G. Fane, Characteristics and potential applications of a novel forward osmosis hollow fiber membrane, *Desalination* 261 (2010) 365–372, <https://doi.org/10.1016/j.desal.2010.06.027>.
- [47] C.H. Tan, H.Y. Ng, Modified models to predict flux behavior in forward osmosis in consideration of external and internal concentration polarizations, *J. Memb. Sci.* 324 (2008) 209–219, <https://doi.org/10.1016/j.memsci.2008.07.020>.
- [48] M.F. Gruber, C.J. Johnson, C.Y. Tang, M.H. Jensen, L. Yde, C. Hélix-Nielsen, Computational fluid dynamics simulations of flow and concentration polarization in forward osmosis membrane systems, *J. Memb. Sci.* 379 (2011) 488–495, <https://doi.org/10.1016/j.memsci.2011.06.022>.
- [49] M. Gulied, A. Al Nouss, M. Khraish, F. AlMomani, Modeling and simulation of fertilizer drawn forward osmosis process using Aspen Plus-MATLAB model, *Sci. Total Environ.* 700 (2020), 134461, <https://doi.org/10.1016/j.scitotenv.2019.134461>.
- [50] S.M. Ali, J.E. Kim, S. Phuntsho, A. Jang, J.Y. Choi, H.K. Shon, Forward osmosis system analysis for optimum design and operating conditions, *Water Res.* 145 (2018) 429–441, <https://doi.org/10.1016/j.watres.2018.08.050>.
- [51] J. Lee, N. Ghaffour, Predicting the performance of large-scale forward osmosis module using spatial variation model: effect of operating parameters including temperature, *Desalination* 469 (2019), 114095, <https://doi.org/10.1016/j.desal.2019.114095>.
- [52] Z.M. Binger, A. Achilli, Forward osmosis and pressure retarded osmosis process modeling for integration with seawater reverse osmosis desalination, *Desalination* 491 (2020), 114583, <https://doi.org/10.1016/j.desal.2020.114583>.
- [53] M. Kumar, M. Grzelakowski, J. Zilles, M. Clark, W. Meier, Highly permeable polymeric membranes based on the incorporation of the functional water channel protein Aquaporin Z, *Proc. Natl. Acad. Sci.* 104 (2007) 20719–20724.
- [54] J. Parodi, J.R. Mangado, O. Stefanson, M. Flynn, H. Shaw, D. Beeler, FOST 2 Upgrade With Hollow-fiber CTA FO Module and Generation of Osmotic Agent for Microorganism Growth Studies, 2016.
- [55] S. Atkinson, De.mem – poised to enter lucrative FO market for dewatering applications, *Membr. Technol.* 2018 (2018) 9–10, [https://doi.org/10.1016/S0958-2118\(18\)30165-4](https://doi.org/10.1016/S0958-2118(18)30165-4).
- [56] R. Wang, L. Shi, C.Y. Tang, S. Chou, C. Qiu, A.G. Fane, Characterization of novel forward osmosis hollow fiber membranes, *J. Memb. Sci.* 355 (2010) 158–167, <https://doi.org/10.1016/j.memsci.2010.03.017>.
- [57] S. Zhao, J. Minier-Matar, S. Chou, R. Wang, A.G. Fane, S. Adham, Gas field produced/process water treatment using forward osmosis hollow fiber membrane: membrane fouling and chemical cleaning, *Desalination* (2017), <https://doi.org/10.1016/j.desal.2016.10.006>.
- [58] N. Singh, I. Petrinic, C. Hélix-Nielsen, S. Basu, M. Balakrishnan, Concentrating molasses distillery wastewater using biomimetic forward osmosis (FO) membranes, *Water Res.* 130 (2018) 271–280, <https://doi.org/10.1016/j.watres.2017.12.006>.
- [59] M. Xie, W. Luo, H. Guo, L.D. Nghiem, C.Y. Tang, S.R. Gray, Trace organic contaminant rejection by aquaporin forward osmosis membrane: transport mechanisms and membrane stability, *Water Res.* 132 (2018) 90–98, <https://doi.org/10.1016/j.watres.2017.12.072>.
- [60] M. Nasser, S. Adham, A. Benamor, S.J. Judd, Osmotic concentration for reducing wastewater injection volumes in Qatar - NPRP10-0118-170191, *Qatar Natl. Res. Fund.* (2018) (Accessed June 7, 2020), <https://mis.qgrants.org/Public/AwardDetails.aspx?ParamPid=fghcebbhdb>.
- [61] R.M. Reynolds, Physical oceanography of the Gulf, Strait of Hormuz, and the Gulf of Oman—results from the Mt Mitchell expedition, *Mar. Pollut. Bull.* 27 (1993) 35–59.
- [62] H.D. Ibrahim, E.A.B. Eltahir, Impact of brine discharge from seawater desalination plants on Persian/Arabian gulf salinity, *J. Environ. Eng.* 145 (2019), 4019084.
- [63] N. Her, G. Amy, D. Foss, J. Cho, Y. Yoon, P. Kosenka, Optimization of method for detecting and characterizing NOM by HPLC—Size exclusion chromatography with UV and on-line DOC detection, *Environ. Sci. Technol.* 36 (2002) 1069–1076, <https://doi.org/10.1021/es015505j>.
- [64] J. Feher, J. Feher, Osmosis and osmotic pressure, *Quant. Hum. Physiol.* (2017) 182–198, <https://doi.org/10.1016/B978-0-12-800883-6.00017-3>.
- [65] K.S. Pitzer, J.C. Peiper, R.H. Busey, K.S. Pitzer, J.C. Peller, Thermodynamic properties of aqueous sodium chloride solutions thermodynamic properties of aqueous sodium chloride solutions, *J. Phys. Chem. Ref. Data* 1 (1992), <https://doi.org/10.1063/1.555709>.
- [66] C.C. Miller, The Stokes-Einstein law for diffusion in solution, *Proc. R. Soc. London. Ser. A, Contain. Pap. a Math. Phys. Character.* 106 (1924) 724–749.
- [67] Y. Marcus, Ionic radii in aqueous solutions, *Chem. Rev.* 88 (1988) 1475–1498.
- [68] H. Ozbek, J.A. Fair, S.L. Phillips, Viscosity Of Aqueous Sodium Chloride Solutions From 0-1500 C, 1977.
- [69] Z. Li, R.V. Linares, S. Bucs, L. Fortunato, C. Hélix-Nielsen, J.S. Vrouwenvelder, N. Ghaffour, T. Leiknes, G. Amy, Aquaporin based biomimetic membrane in forward osmosis: chemical cleaning resistance and practical operation, *Desalination* 420 (2017) 208–215.
- [70] M.S. Camilleri-Rumbau, J.L. Soler-Cabezas, K.V. Christensen, B. Norddahl, J. A. Mendoza-Roca, M.C. Vincent-Vela, Application of aquaporin-based forward osmosis membranes for processing of digestate liquid fractions, *Chem. Eng. J.* 371 (2019) 583–592, <https://doi.org/10.1016/j.cej.2019.02.029>.
- [71] M. Sauchelli, G. Pellegrino, A. D'Haese, I. Rodríguez-Roda, W. Gernjak, Transport of trace organic compounds through novel forward osmosis membranes: role of membrane properties and the draw solution, *Water Res.* 141 (2018) 65–73, <https://doi.org/10.1016/j.watres.2018.05.003>.
- [72] S. Zou, M. Qin, Z. He, Tackle reverse solute flux in forward osmosis towards sustainable water recovery: reduction and perspectives, *Water Res.* 149 (2019) 362–374, <https://doi.org/10.1016/j.watres.2018.11.015>.
- [73] J.-Y. Li, Z.-Y. Ni, Z.-Y. Zhou, Y.-X. Hu, X.-H. Xu, L.-H. Cheng, Membrane fouling of forward osmosis in dewatering of soluble algal products: comparison of TFC and CTA membranes, *J. Memb. Sci.* 552 (2018) 213–221.
- [74] G. Blandin, H. Vervoort, P. Le-Clech, A.R.D. Verliefde, Fouling and cleaning of high permeability forward osmosis membranes, *J. Water Process Eng.* 9 (2016) 161–169.
- [75] M. Li, K. Li, L. Wang, X. Zhang, Feasibility of concentrating textile wastewater using a hybrid forward osmosis-membrane distillation (FO-MD) process: performance and economic evaluation, *Water Res.* 172 (2020), 115488, <https://doi.org/10.1016/j.watres.2020.115488>.
- [76] S.A. Huber, A. Balz, M. Abert, W. Pronk, Characterisation of aquatic humic and non-humic matter with size-exclusion chromatography–organic carbon detection–organic nitrogen detection (LC-OCD-OND), *Water Res.* 45 (2011) 879–885.